Supplementary Information (SI) for Sustainable Energy & Fuels.

Supplementary Materials

Two-dimensional h-BAs/MoXTe (X=S, Se) heterojunctions with high photocatalytic performance and high photoelectric conversion efficiency

S1. The geometric structures and band structures of h-BAs, MoSTe, and MoSeTe monolayers

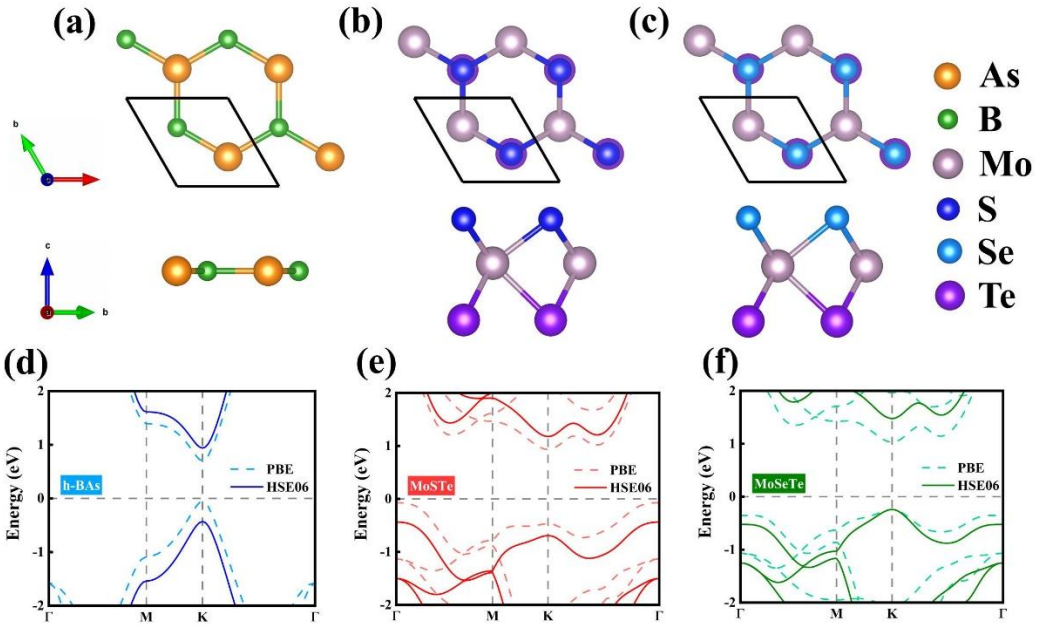

Fig. S1. Top and side views of the geometric structures of the (a) h-BAs, (b) MoSTe, and (c) MoSeTe monolayers. Orange, green, pink, blue, cyan, and purple balls represent As, B, Mo, S, Se, and Te atoms, respectively. Band structures of the (d) h-BAs, (e) MoSTe, and (f) MoSeTe monolayers obtained by the PBE and HSE06 functional.

Fig. S1(a-c) show the top and side views of the optimized geometric structures of h-BAs, MoSTe, and MoSeTe monolayers, respectively. It can be found that the three monolayers are hexagonal crystal structures. After structural optimization, the lattice constants of h-BAs, MoSTe, and MoSeTe monolayers are 3.39 Å, 3.37 Å, and 3.44 Å, respectively. The results show

that the B-As bond length is 1.96 Å, while the bond lengths of Mo-S, Mo-Se, and Mo-Te are 2.44 Å, 2.56 Å, and 2.72 Å. In addition, the band structures of h-BAs, MoSTe, and MoSeTe monolayers were calculated, as shown in Fig. S1(d-f). According to the calculations of the HSE06 (PBE) functional, the bandgap values of h-BAs, MoSTe, and MoSeTe monolayers are 1.37 eV (0.75 eV), 1.62 eV (1.02 eV), and 1.72 eV (1.27 eV), respectively. It can be found that the h-BAs and MoSeTe monolayers are direct bandgap semiconductors, while the MoSTe is indirect bandgap.

S2. The stacking structural models of h-BAs/MoXTe heterojunctions

As shown in Fig. S2(a-l), we designed twelve different stacking structures for h-BAs/MoSTe heterojunctions. In order to distinguish the different structures of the heterojunctions, the twelve configurations were classified into AA, AA', AB, and AB' stacking types. Among them, the AA (AA') stacking type is that h-BAs layer is adjacent to the Te atomic layer of MoSTe, and the AB (AB') stacking type is that h-BAs layer is adjacent to the S atomic layer of MoSTe. The AA (AB) and AA' (AB') stacking types can be converted to each other by rotating the h-BAs layer horizontally by 180°. It can be found that each stacking type contains three different configurations. For AA stacking type, there are AA-1, AA-2, and AA-3 configurations, which can be transformed into each other by horizontally moving the upper MoSTe layer. The AA-1 configuration is that the S (Te) and Mo atoms in the upper layer cover the As and B atoms in the lower layer, respectively. The AA-2 configuration is that the upper Mo atoms cover the lower As atoms and the S (Te) atoms are located on the lattice edges. While the AA-3 configuration is that the upper S (Te) atoms cover the lower B atoms and the Mo atoms are located on the lattice edges. For the AA', AB, and AB' stacking types, their configurations are named in a manner similar to that of the configurations of the AA stacking type.

Similarly, twelve different stacking structures for h-BAs/MoSeTe heterojunctions were designed, as shown in Fig. S3(a-l). We classified these configurations into AC, AC', AD, and AD' stacking types. For h-BAs/MoSeTe heterojunctions, the configurations of the different stacking types are named in a similar way to the above naming of h-BAs/MoSTe

heterojunctions.

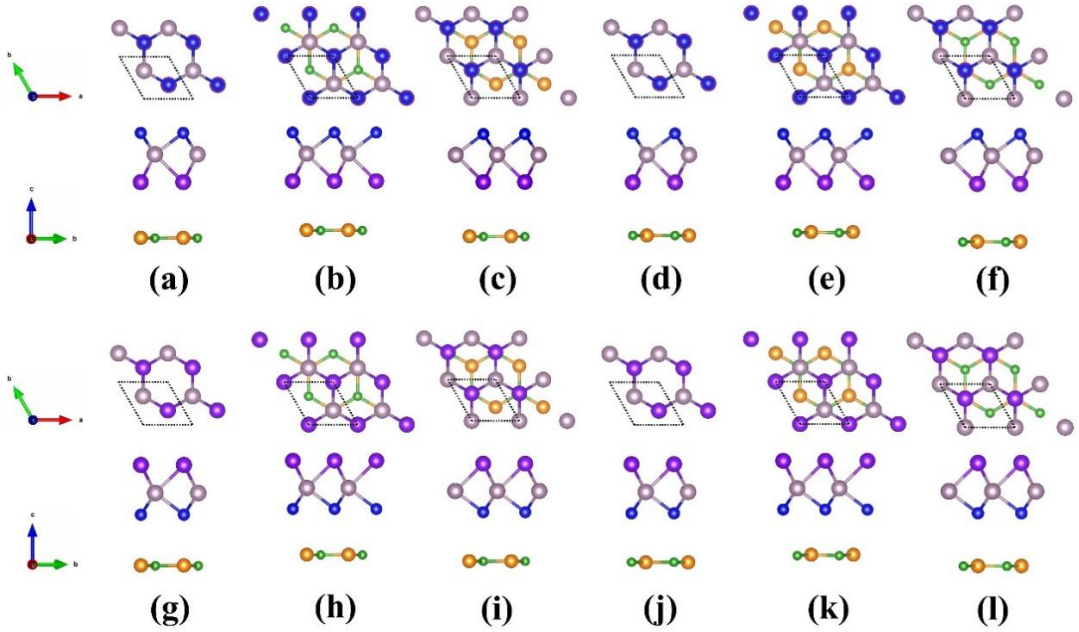

Fig. S2. Top and side views of the stacking structures of h-BAs/MoSTe heterojunctions. (a) AA-1; (b) AA-2; (c) AA-3; (d) AA'-1; (e) AA'-2; (f) AA'-3; (g) AB-1; (h) AB-2; (i) AB-3; (j) AB'-1; (k) AB'-2; (l) AB'-3. Green, orange, pink, blue, and purple represent B, As, Mo, S, and Te atoms, respectively.

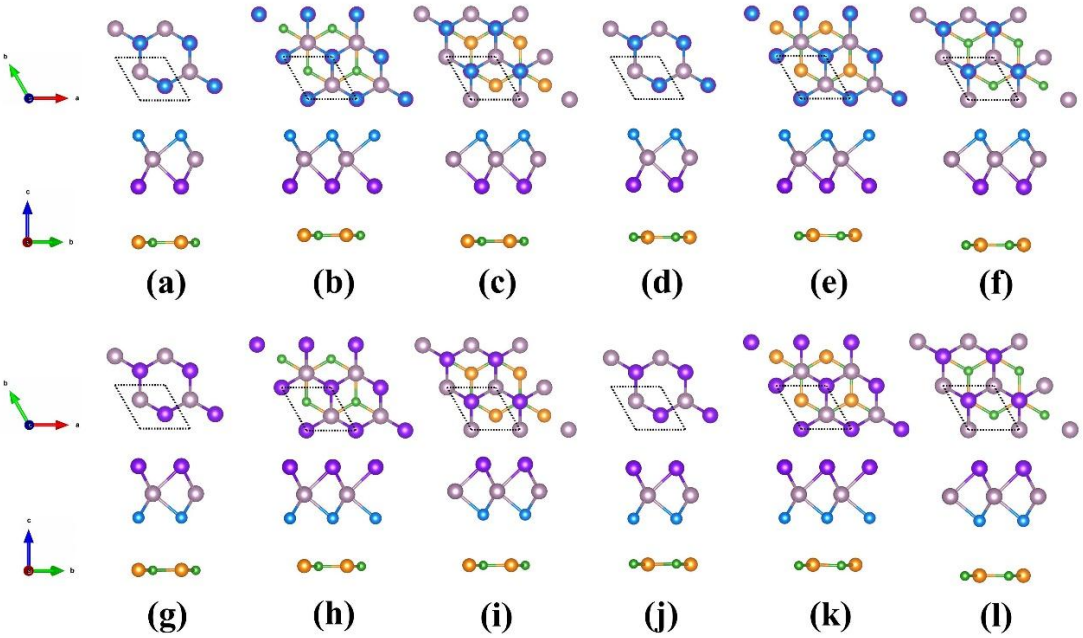

Fig. S3. Top and side views of the stacking structures of h-BAs/MoSeTe heterojunctions. (a) AC-1; (b) AC-2; (c) AC-3; (d) AC'-1; (e) AC'-2; (f) AC'-3; (g) AD-1; (h) AD-2; (i) AD-3; (j) AD'-1; (k) AD'-2; (l) AD'-3. Green, orange, pink, cyan, and purple represent B, As, Mo, Se, and Te atoms, respectively.

Table. S1. Lattice constants (a), interlayer distances (d), and formation energy (E_f) of the h-BAs/MoXTe heterojunctions.

Structure	a (Å)	d (Å)	E_f (eV)	Structure	a (Å)	d (Å)	E_f (eV)
AA-1	3.35	3.80	-1.52	AC-1	3.38	3.81	-1.57
AA-2	3.35	3.41	-1.60	AC-2	3.38	3.77	-1.68
AA-3	3.35	3.83	-1.52	AC-3	3.38	3.79	-1.57
AA'-1	3.35	3.65	-1.55	AC'-1	3.38	3.65	-1.59
AA'-2	3.35	3.43	-1.59	AC'-2	3.38	3.42	-1.64
AA'-3	3.35	3.90	-1.51	AC'-3	3.38	3.91	-1.55
AB-1	3.35	3.43	-1.52	AD-1	3.38	3.56	-1.57
AB-2	3.35	3.18	-1.57	AD-2	3.38	3.25	-1.62
AB-3	3.35	3.40	-1.53	AD-3	3.38	3.53	-1.57
AB'-1	3.35	3.34	-1.54	AD'-1	3.38	3.10	-1.57
AB'-2	3.35	3.12	-1.58	AD'-2	3.38	3.22	-1.63
AB'-3	3.35	3.53	-1.51	AD'-3	3.38	3.65	-1.55

S3. Band structures of h-BAs/MoXTe heterojunctions

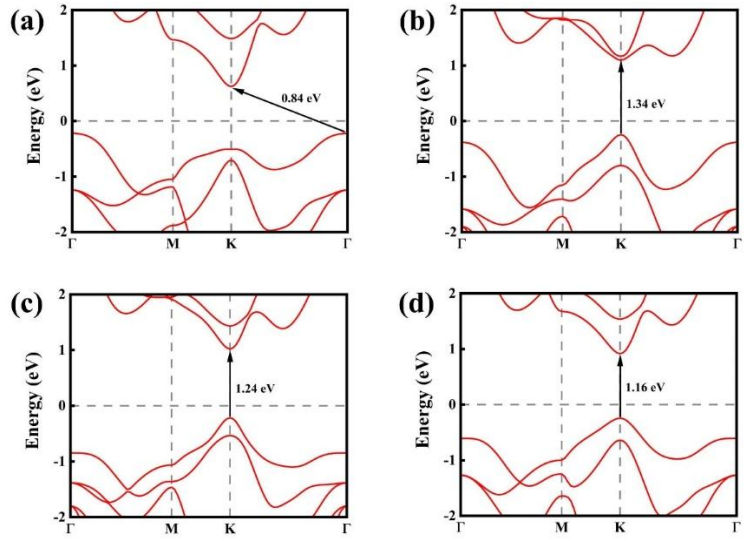

Fig. S4. Band structures of (a) h-BAs/TeMoS, (b) h-BAs/SMoTe, (c) h-BAs/TeMoSe, and (d) h-BAs/SeMoTe heterojunctions.

S4. Electrostatic potential of monolayers

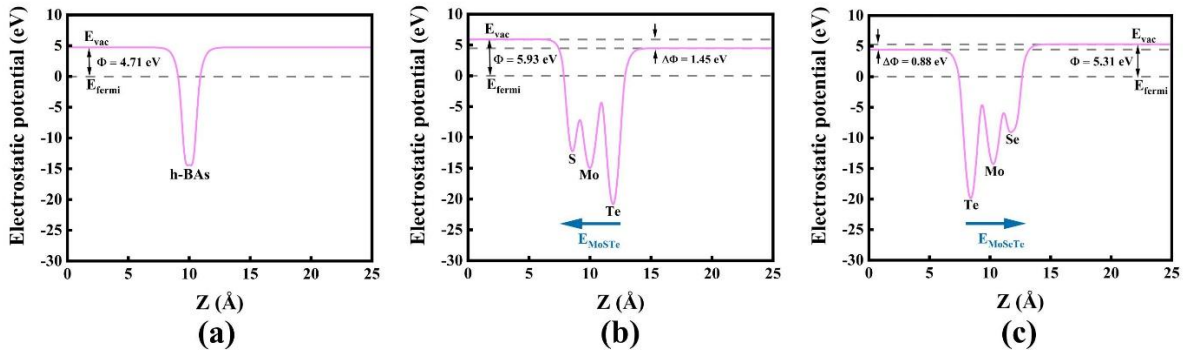

Fig. S5. Electrostatic potential along the z-direction of (a) h-BAs, (b) MoSTe, and (c) MoSeTe monolayers. The blue arrows stand for intrinsic electric field of Janus layer.

S5. Band edge positions of monolayers and the redox potential of water at different pH

As shown in Fig S6, the band edge positions of h-BAs monolayer can meet the redox potentials for overall water splitting in the pH range of 8~10. MoSTe monolayer can only complete the oxidation of water. While for MoSeTe monolayer, the pH value range of redox potentials of water included in its band edge positions is 4~11.

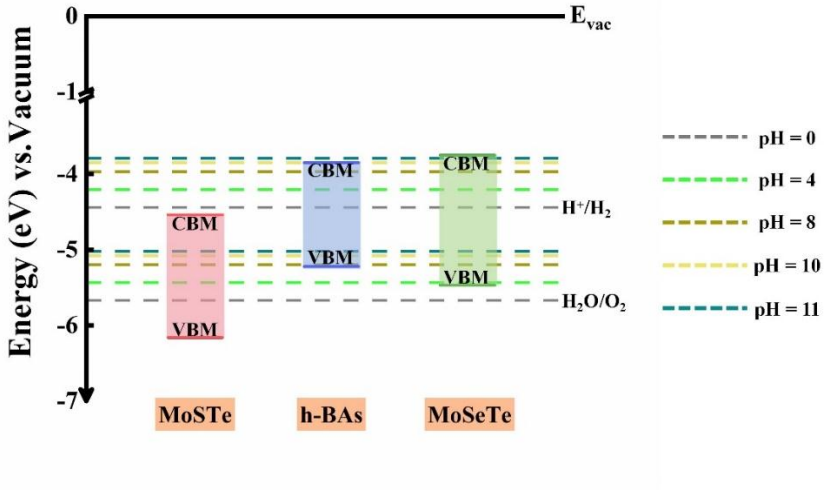

Fig. S6. Band edge positions of the isolated h-BAs, MoSTe, and MoSeTe monolayers referring to the vacuum level. The vacuum level is set to zero. The dashed lines with different colors represent the redox potential of water at different pH.